Research on Fault Diagnosis Algorithm of Substation Equipment Based on Improved Mask R-CNN

Yang Yang[*1], Diao Guanxun[2], Yang Ning[1], Wang Mei[2], Jia Pengfei[1], Qian Chengchen[2], Li Lihua[1]

[*1]China Electric Power Research Institute, No. 15 Xiaoyingdonglu, Beijing, China
E-mail: yang.yang_epri@qq.com
[2] Shanghai Electric Power Company Maintenance Company, No. 620 Wuning Road, Shanghai, China
E-mail: 1458172995@qq.com

Abstract. Electric power networks are composed of various electrical equipment. Any equipment failures can affect the stable operation of the electric networks. By analyzing the infrared images of substation equipment, equipment defects can be found in time to prevent malfunctions effectively. This paper proposes an infrared image fault diagnosis algorithm for substation equipment based on the improved Mask R-CNN. Attention mechanism is introduced into the feature extraction network, and the anchor ratios are modified. Firstly, the improved Mask R-CNN is applied to detect and segment the target equipment, including lightning arresters, current transformers side bushings, current transformers, and voltage transformers. Then the temperature is extracted from the infrared image. Finally, the relative temperature difference method is used to determine the fault type and seriousness. The original method and the proposed method were compared in aspects of split effect and temperature anomaly diagnosis. Experimental results show that the IoU (Intersection over Union) of proposed algorithm improves 6.08% compared with original method.

Keywords: Substation equipment; infrared image; attention mechanism; image segmentation; fault diagnosis

1. INTRODUCTION

Electric power substations are important parts of the electric power system. The stable operation of the substation equipment is directly related to the safety and stability of electric grids. Infrared thermal imaging technology has been widely applied in substations for fault diagnosis of substation equipment with the advantages of no contact and no power outage [1-2]. Electric power equipment is usually accompanied by heating during operation, and the degree of temperature rise will directly reflect the operating state of the equipment. Therefore, temperature monitoring of electric power equipment is an indispensable work in the state assessment. The application of infrared imaging technology in the field of electric power equipment is produced under this background. Compared with visible light imaging technology, infrared imaging technology can not only get the contour information of the device, but also the temperature information of the device. The use of infrared diagnostic technology in the condition monitoring and equipment maintenance of substations can identify equipment defects that are difficult to find only by the naked eye as soon as possible, and eliminate them in time to avoid their continuous deterioration and cause more serious accidents. Li et al [3] proposed an infrared image defect recognition method for substation equipment based on Faster RCNN, but the segmented area contains background information; Wu et al [4] proposed an image segmentation technology for power equipment based on Mask R-CNN. The segmentation effect is good, but the required training samples are larger. Mo et al [5] proposed a research and implementation of infrared image segmentation technology for power equipment based on Mask R-CNN. They improved the deficiencies of the Mask R-CNN framework in the image segmentation part by fusing low-level feature information, but the number of training samples required is also larger. Yang et al [6] proposed a research on the power equipment state detection algorithm for inspection robots based on YOLOv3, which achieved lightweight, but the detection effect was not improved. Chen Da et al. [7] proposed a fault diagnosis method for power equipment based on deep learning, and used MobileNet to perform fault diagnosis on infrared images of equipment, but this method has errors in the temperature extraction process. Different from the previous fault diagnosis methods, the fault diagnosis algorithm proposed in this paper includes target segmentation and fault diagnosis. The improvement method proposed in this paper is as follows. In the target segmentation link, aiming at the problem of few infrared image samples of substation equipment, the method of transfer learning is introduced, and the number of samples is expanded by graying the image. Aiming at the problem of the low segmentation based on Mask R-CNN, a method combining the attention mechanism and Mask R-CNN is proposed. Then in the RPN (Region Proposal Network) generation anchor stage, according to the characteristics of the substation equipment, the basic anchor ratio is improved. In the fault diagnosis link, this paper proposes a method combining Mask R-CNN and temperature matrix. Firstly, device temperature is extracted, and then the relative temperature difference method is used to diagnose the fault. Take the current transformer as an example to compare the fault diagnosis effect of the improved method and the original method.

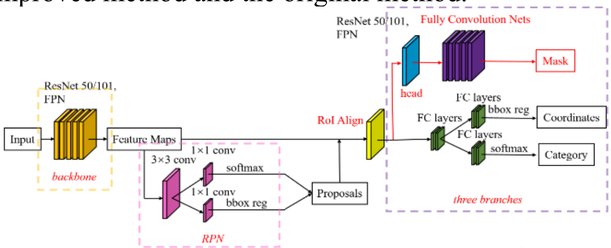

Fig. 1 Mask R-CNN structure diagram

2. TARGET SEGMENTATION AND FAULT DIAGNOSIS

2.1. Introduction to Mask R-CNN

Mask R-CNN is an instance segmentation framework proposed by He et al [8] in 2017. This method adds the Mask branch on the basis of Faster R-CNN [9], and performs pixel-level target detection，segmentation and classification at the same time. It replaces the ROI (Region of Interest) pooling in Faster R-CNN with ROI align, which solves the regional misalignment problem with higher accuracy and speed. Compared with traditional target detection methods, applying Mask R-CNN to the segmentation of substation equipment can not only improve the accuracy of target detection, but also remove background information and better extract the equipment area.

2.1.1. Mask R-CNN Structure

The structure of Mask R-CNN is shown in Figure 1, and its network is composed of three parts: backbone, RPN [10], and ROI Head. The backbone is a series of convolutional layers used to extract the feature map of the images, such as ResNet50 and ResNet101. RPN is a regional recommendation network, which is used to help the network recommend areas of interest. The area scanned by the RPN is called an anchor, which is a rectangle distributed on the image area. ROI Head is divided into RoI Box Head and RoI Mask Head.

2.1.2. Mask R-CNN loss function

The loss in the deep neural network is used to measure the gap between the predicted value of our model and the true value of the data. The purpose of model training is to optimize the parameters in the model to reduce the loss value. The Mask branch generates an output feature map for each ROI area. The calculation formula of the loss function of Mask R-CNN is as follows：

$$Loss = L_{cls} + L_{box} + L_{mask} \tag{1}$$

Where L_{cls} and L_{box} use full connection to predict the category of each RoI and the coordinate value of its rectangular frame. L_{cls} is the classification loss function, Set p_i as the probability value corresponding to the correct classification, and select the cross entropy as the measurement standard. The calculation formula is:

$$L_{cls} = -0.005 \times \sum_{i=1}^{200} \begin{matrix}[p_i \log(p_i) + \\ (1-p_i)\log(1-p_i)]\end{matrix} \tag{2}$$

Where L_{box} is the regression loss function, the calculation formula is:

$$L_{box} = 0.005 \times \sum_{i=1}^{200} \begin{matrix}[f(dx_t, dx_p) \\ + f(dy_t, dy_p) \\ + f(dw_t, dw_p) \\ + f(dh_t, dh_p)]\end{matrix} \tag{3}$$

$$f(a,b) = \begin{Bmatrix} 0.5 \times (a-b)^2, if\,|x| < 1 \\ |a-b| - 0.5, otherwise \end{Bmatrix} \tag{4}$$

Where L_{mask} is the regression loss function, and its calculation formula is:

$$L_{mask} = \frac{\sum_{i=1}^{200}\sum_{j=1}^{28\times 28} \cos t(y_j, p(y_j \mid x_j))}{200} \tag{5}$$

$$\begin{aligned} &\cos t(y, p(y)) = -y \ln p(y \mid x) \\ &-(1-y)\ln(1-p(y \mid x)) \end{aligned} \tag{6}$$

2.2. Relative temperature difference

The relative temperature difference discrimination method is based on the People's Republic of China Electric Power Industry Standard DL/T 664-2016[11]. The definition of relative temperature difference is as follows:

$$\begin{aligned} \delta_t &= (\tau_1 - \tau_2)/\tau_1 \times 100\% \\ &= (T_1 - T_2)/(T_1 - T_0) \times 100\% \end{aligned} \tag{7}$$

Formula:

τ_1 and T —The temperature rise and temperature of the hot spot.

τ_2 and T_2 —The temperature rise and temperature of the normal corresponding point.

T_0—The ambient temperature-air temperature in the area of the device under test.

The guideline judgment standard is converted into an executable logic expression, taking the current transformer as an example. As shown in Table 1.

3. IMPROVED MASK R-CNN

In order to realize the fault diagnosis of the infrared image of the substation equipment, it is necessary to obtain the temperature information of the equipment area. In order to better extract the temperature information of the equipment area, this paper combines the Mask R-CNN algorithm with the temperature matrix, and proposes the Mask-MOT (matrix of temperature) model.

Table. 1 Caption for table

Nature of defect	Diagnose based on	Diagnosis rules
Critical defect	Hot spot temperature >80°C	JTX[Max]>=80
	δ≥95% and Hot spot temperature >55°C	(JTX[Max]-JTY[Max])/(JTX[Max]-T0)>=0.95 and JTX[Max]>55
Serious defect	80°C≥Hot spot temperature >55°C	80>=JTX[Max]>55
	δ≥80% but the hot spot temperature does not reach the critical defect temperature value	(JTX[Max]-JTY[Max])/(JTX[Max]-T0)>=0.8 and JTX[Max]<80
General defect	δ≥35% but the hot spot temperature did not reach the critical defect temperature value	(JTX[Max]-JTY[Max])/(JTX[Max]-T0)>=0.35and JTX[Max]<=55

3.1. Mask-MOT model

The structure of the Mask-MOT model is shown in Figure 2. Firstly, the infrared image is obtained by the Mask R-CNN algorithm to obtain the segmented area of the device to generate the Mask matrix; then the FLIR tool is used to obtain the temperature matrix of the infrared image.

The dimensions of the Mask matrix and the temperature matrix are the same. Let the Mask matrix be mask, the temperature matrix be data, and the temperature matrix of the segmented area be Seg. The value of the mask matrix corresponding to the segmented area of the infrared image is True, and the value of the mask matrix corresponding to the other areas is False. The temperature matrix of the segmented area is obtained by mapping the pixels with the value of True in the mask matrix to the temperature matrix.

The key of the fault diagnosis algorithm lies in the precise segmentation of the equipment area. The traditional Mask R-CNN algorithm is used to segment the infrared images of substation equipment, but the segmented contours are quite different from the actual contours. There are two reasons for the poor segmentation effect: one is that ResNet, the basic network of Mask R-CNN, does not make full use of image information; the other is that the basic anchor aspect ratio of the traditional Mask R-CNN algorithm is set for public data sets, it does not apply to substation equipment.

3.2. Improved feature extraction network

3.2.1. SENet Structure

SENet (Squeeze-and-excitation network) is a new network structure proposed by Hu et al. [12] in 2017. SENet mainly learns the correlation between channels in the convolution process, and it filters out channel-based attention. The realization process is shown in Figure 3. SENet learns a set of weight coefficients through a small fully connected network, and it weights each channel of the original feature map. In this way, each sample (including training samples and test samples) has its own unique set of weights for the weighting of its own feature channels. This is actually an attention mechanism, that is, paying attention to important feature channels and then giving them a higher weight.

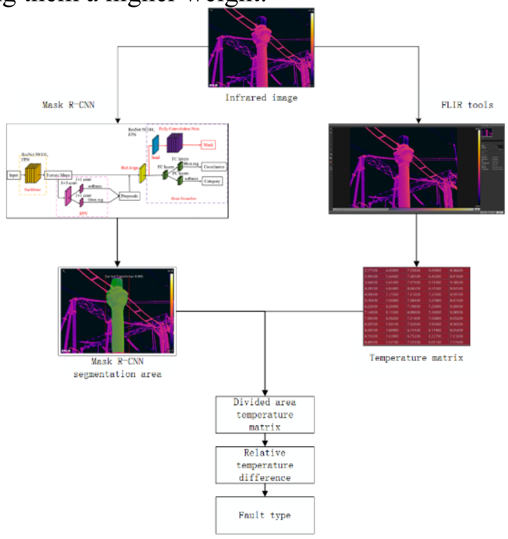

Fig. 2 Mask-MOT model

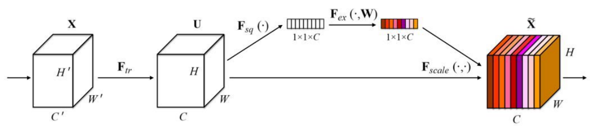

Fig. 3 SENet structure diagram

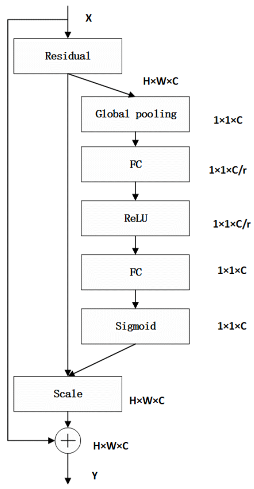

Fig. 4 SE-ResNet structure diagram

3.2.2 ResNet embedded with SEnet

This article embeds SENet in ResNet, and its structure is shown in Figure 4. First, the feature dimension is reduced to 1/r of the input, and then it is activated by ReLu and then raised back to the original dimension through a Fully Connected layer.

The model is trained in a way that the weight of important feature information is large and the weight of other feature information is small [13], and the steps are as follows:

1) Squeeze operation: Perform global average pooling on the convolutional eigenvalues, and compress the entire channel into a channel description symbol, that is z_c, the calculation formula is as follows:

$$z_c = \frac{1}{H \times W} \sum_{i=1}^{H} \sum_{j=1}^{W} u_c(i, j) \tag{8}$$

2) Excitation operation: After a fully connected layer output feature, use the ReLU function to activate; then through a fully connected layer output feature, use the Sigmoid function to activate the feature, and generate the weight information corresponding to each channel. The calculation formula is as follows:

$$s = \sigma(W_2 \delta(W_1 z)) \tag{9}$$

Where s represents the set of weights of each channel, δ Represents the ReLU function, σ represents the Sigmoid activation function, and represents the set of real numbers obtained by the excitation operation of each channel, W_1 and W_2 are obtained through learning.

3.3. Improved the regional proposal network

The shape of the substation equipment is mostly slender. In the traditional Mask R-CNN algorithm, the aspect ratio of the anchor is (1:2, 1:1, 2:1). This ratio is not suitable for slender targets. To identify, the aspect ratio of the anchor needs to be improved. In this paper, according to the principle of RPN generation of basic anchors, statistics on the aspect ratio of the equipment in the infrared image data of the substation equipment [14], the statistical results are shown in Figure 5, where the range of the aspect ratio of the substation equipment is in order of quantity The order is (4:1, 3:1, 5:1, 2:1). According to the statistics of the aspect ratio of substation equipment, change the aspect ratio of the anchor to (3:1,4:1,5:1).

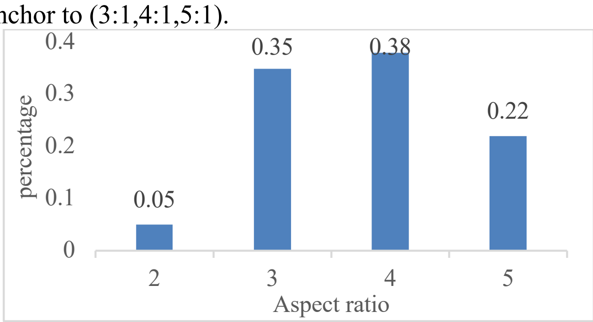

Fig. 5 Percentage statistics of aspect ratio of substation equipment

Table. 2 Comparison of Evaluation Indexes of Mask R-CNN Segmentation Results Before and After Improvement

Model	IoU_{Mask}/%					
	TLA	FLA	CT	VT	CTSB	ALL
Original Model	80.6	62.5	88.9	82.9	86.8	80.34
Improve Model	88.2	75.6	90.7	88.4	89.2	86.42

4. Experiment and Result Analysis

The experimental hardware environment of this article is: Intel(R) i7-6850K, GeForce GTX 1080 Ti; the software environment is: Ubuntu16.04, TensorFlow-GPU1.13.1, Keras2.2.4, CUDA10.0.13, Cudnn7.6.4.

4.1. Infrared image data set of substation equipment

Two kinds of lightning arresters, rheological side bushings, current transformers, voltage transformers were selected, and a total of 317 pictures of five substation equipment for target detection, including 272 training pictures and 45 test pictures. The training samples were expanded by graying the training pictures, and 544 training pictures were obtained.

4.2. Evaluation of target segmentation performance

This paper draws on the practice in the literature [15] and selects the IoU value to evaluate the mask quality. Quantify the quality of Mask segmentation by calculating the ratio of intersection and union between the mask area (F) predicted by the segmentation algorithm and the mask area (G) that is manually labeled. The IoU value is calculated as follows:

$$\mathrm{IoU}_{\mathrm{Mask}} = \frac{Mask(F) \cap Mask(G)}{Mask(F) \cup Mask(G)} \tag{9}$$

4.3. Experimental results

4.3.1. Segmentation results

In order to verify the effectiveness of the improved Mask R-CNN model in substation equipment segmentation, the improved model and the original Mask R-CNN model are compared on the test set of substation equipment mentioned above. The improved model is in the original Mask R -Based on the CNN network, the feature extraction network structure and anchor value are optimized at the same time. The parameter settings during the training process are consistent with the original Mask R-CNN network. The segmentation evaluation indices obtained are shown in Table 2. Where TLA represents No. 3 main transformer arrester, FLA represents No. 4 main transformer arrester, CT represents current transformer, VT represents voltage transformer, and CTSB represents rheological side bushing. The improved segmentation effect is shown in Figure 6. Figure 6 (a)-(e) are the segmentation results of the original model, Figure 6 (f)- (j) are the segmentation results of the improved model.

The IoU Mask of the improved Mask R-CNN reaches 86.4%, which is a significant improvement compared to the original Mask R-CNN model. Among them, the surge arrester of No. 3 main transformer increased by 7.6%, the surge arrester of No. 4 main transformer increased by 13.1%, rheology increased by 1.8%, voltage transformer increased by 5.5%, rheological side casing increased by 2.4%, and the overall average increase was 6.08%.

4.3.2. Fault diagnosis results

Use the fault diagnosis algorithm proposed in this paper to diagnose the fault of the substation equipment, input the infrared picture of the substation equipment and the corresponding temperature matrix, and the output result is shown in Figure 7, Figure 7 (a) is the improved diagnosis result, Figure 7 (b) It is the diagnosis result before improvement. The actual relative temperature difference of the current transformer is 0.355, and the fault type is general fault. For the improved diagnosis algorithm, according to the fault diagnosis algorithm, the relative temperature difference of the equipment is calculated to be 0.357, which is larger than 0.35, thus there is a general fault. For the diagnosis algorithm before improvement, the relative temperature difference of the equipment is calculated to be 0.502>0.35, and the equipment is a general fault. Although the diagnosis results of the two methods are general faults, the relative temperature difference calculated by the improved diagnosis method is more accurate.

4.4. Analysis of influencing factors

In order to show the impact of each improvement on the performance of the model, this section compares the model with only the anchor and only the SEnet with the original Mask R-CNN network model under the same training parameters and data set. Under the same conditions, the model with only the anchor and the original Mask R-CNN model were compared and tested on three basic networks: Vgg16, ResNet50 and ResNet101. The segmentation effect is shown in Figure 8.The results are shown in Table 3.

By changing the anchor aspect ratio, the model improves on the IoU Mask of different basic networks. The Vgg16 network is increased by 1.84%. Where the No. 3 main transformer arrester has increased by 2%, the No. 4 main transformer arrester has increased by 1.7%, the current transformer has increased by 2.2%, the voltage transformer has increased by 1.6% and the rheological side bushing has increased by 1.7%. The ResNet50 network is increased by 1.8%. Where the No. 3 main transformer arrester has increased by 2.7%, the No. 4 main transformer arrester has increased by 3.3%, the current transformer has increased by 0.5%, the voltage transformer has increased by 1.7% and the rheological side bushing has increased by 0.8%. The ResNet101 network is increased by 2.64%. Where the No. 3 main transformer arrester has increased by 4.2%, the No. 4 main transformer arrester has increased by 5.8%, the current transformer has increased by 0.3%, the voltage transformer has increased by 2.4% and the rheological side bushing has increased by 0.5%. It shows that changing the aspect ratio of the anchor to make it suitable for the slender characteristics of the substation equipment can effectively improve the segmentation effect of the substation equipment.

Under the same conditions, the model with only SEnet and the original Mask R-CNN model were compared and tested on three basic networks: Vgg16, ResNet50 and ResNet101. The segmentation results are shown in Figure 9. The evaluation indices are shown in Table 4.

By adding the attention mechanism, the model has improved on the IoU Mask of different basic networks. Among them, the Vgg16 network increased by 1.96%, the ResNet50 network increased by 2.26%, and the ResNet101 network increased by 2.68%. Which shows that the addition of attention mechanism makes the feature extraction network make full use of channel information and enhance the feature extraction ability of the network, which can effectively improve the segmentation effect of substation equipment.

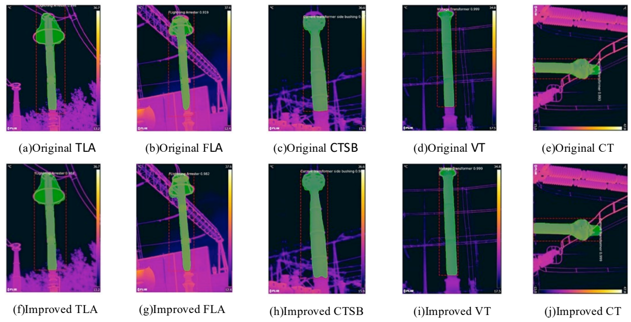

Fig. 6 Comparison of segmentation results by original Mask R-CNN model and improved Mask R-CNN model

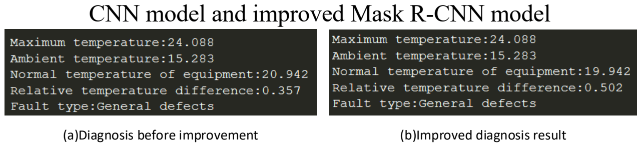

Fig. 7 Diagnosis results before and after improvement

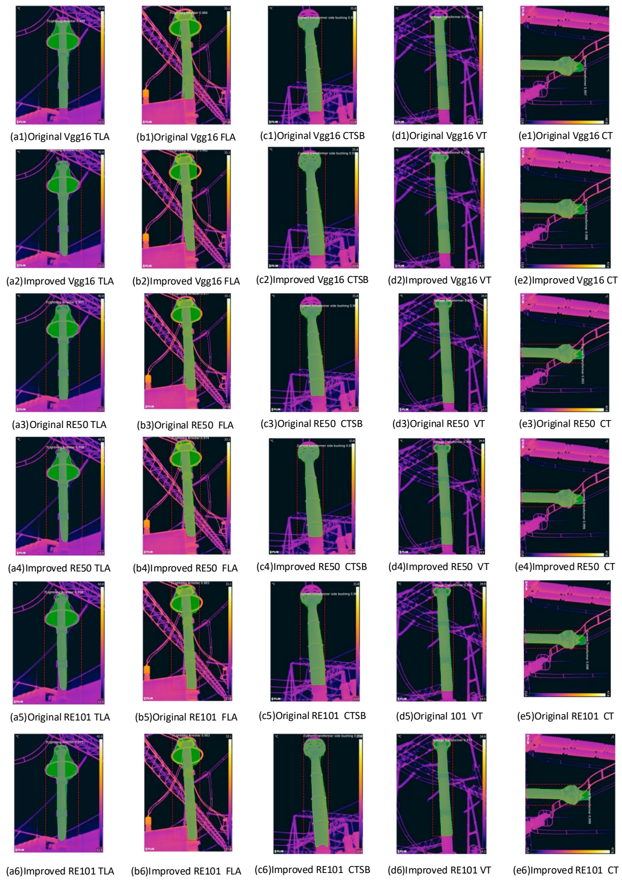

Fig. 8 Different anchor segmentation effects

Table. 3 Comparison of model evaluation indicators before and after changing the anchor

Anchor+ Backbone	IoU_{Mask}					
	TLA	FLA	CT	VT	CTSB	ALL
[1:2,1,2:1]+ Vgg16	79.2	61.5	86.4	80.5	85.2	78.56
[3:1,4:1,5:1]+ Vgg16	81.2	63.2	88.6	82.1	86.9	80.4
[1:2,1,2:1]+ ResNet50	79.6	62.1	88.5	81.6	86.3	79.62
[3:1,4:1,5:1]+ ResNet50	82.3	65.4	89.0	83.3	87.1	81.42
[1:2,1,2:1]+ ResNet101	80.6	62.5	88.9	82.9	86.8	80.34
[3:1,4:1,5:1]+ ResNet101	84.8	68.3	89.2	85.3	87.3	82.98

Table. 4 Comparison of model evaluation indicators before and after adding SENet

Backbone	IoU_{Mask}					
	TLA	FLA	CT	VT	CTSB	ALL
Vgg16	79.2	61.5	86.4	80.5	85.2	78.56
SE-Vgg16	81.8	62.2	87.6	84.3	86.7	80.52
Resnet50	79.6	62.1	88.5	81.6	86.3	79.62
SE-ResNet50	83.6	64.5	89.2	85.2	86.9	81.88
Resnet101	80.6	62.5	88.9	82.9	86.8	80.34
SE-Resnet101	85.8	66.2	89.5	86.5	87.1	83.02

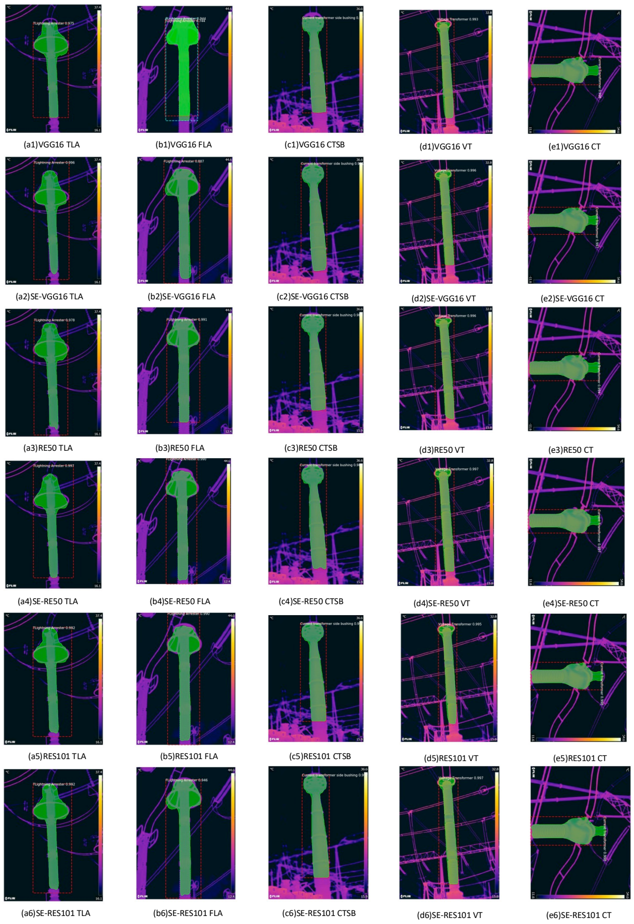

Fig. 9 Attention mechanism segmentation effect

5. Conclusion

This article first uses the improved Mask R-CNN to segment the five types of equipment in the substation. Compared with the original Mask R-CNN algorithm, the improved algorithm can better segment the equipment area. Then, in the segmented infrared image, the temperature of the equipment area is extracted, and the relative temperature difference discrimination method is used to perform the fault diagnosis algorithm. The fault diagnosis algorithm proposed in this paper can improve the automatic diagnosis level of infrared images of substation equipment. Compared with the previous algorithm, the equipment has higher recognition accuracy, better segmentation effect, and fewer training samples are required. The fault diagnosis of substation equipment based on the improved Mask R-CNN has a good development prospect, which can greatly improve the detection efficiency and early warning capability of substation equipment.

Acknowledgement

This work is supported by the Science and Technology Project of State Grid Corporation of China under Grant 5500-202017468A-0-0-00.

References:

[1] Tan, Y. and Fa, S., 2021. Infrared Thermal Image Recognition of Substation Equipment Based on Image Enhancement and Deep Learning. Proceedings of the CSEE, 2021(03):1-10.

[2] Wu J. and Li Y., 2006. Application of Infrared Thermal Image Instrument in Power Equipment Fault Diagnosis. Electrical Equipment, 2006(09):38-41.

[3] Li W., Xie K. and Liao X., 2019. Intelligent Diagnosis Method of Infrared Image for Transformer Equipment Based on Improved Faster RCNN. Southern Power System Technology, 2019(12).

[4] Wu K., Wang M., and Li Y., 2020. Research on Infrared Image Segmentation Technology of Power Equipment Based on Mask R-CNN. Computer & Digital Engineering,2020, 048(002):417-422.

[5] Mo B., 2020. Research and Implementation on Infrared Image Segmentation Technology of Electrical Equipment Based on Mask R-CNN. North China Electric Power University,2020.

[6] Yang X., Li S., Li J., Li S. and Zhang X., 2021. Research on Algorithm for Equipment Condition Monitoring Based on Inspection Robot. Computer Technology and Development, 2021,31(03):201-205-210.

[7] Chen D.,Tang W. and Niu Z., 2021. Fault Diagnosis Method for Power Equipment Infrared I mages Based on Deep Learning. Guangdong Electric Power, 2021,34(01):97-105.

[8] He K., Gkioxari G., Dollár P. and Girshick R., 2017. Mask R-CNN. IEEE Transactions on Pattern Analysis & Machine Intelligence, 2017.

[9] Ren S., He K., Girshick R. and Sun J., 2017. Faster R-CNN: Towards Real-Time Object Detection with Region Proposal Networks. IEEE Transactions on Pattern Analysis & Machine Intelligence, 2017, 39(6):1137-1149.

[10] Lin T., Dollar P., Girshick R., He K., Hariharan B. and Belongie S., 2017. Feature Pyramid Networks for Object Detection. 2017 IEEE Conference on Computer Vision and Pattern Recognition (CVPR). IEEE Computer Society, 2017.

[11] DLT 664-2016 Application Specification for Infrared Diagnosis of Live Equipment.

[12] Jie H., Li S., Gang S. and Albanie S., 2017. Squeeze-and-Excitation Networks. IEEE Transactions on Pattern Analysis and Machine Intelligence, 2017, PP(99).

[13] Li H., Chen G. and Pei A., 2020. Research on individual recognition of dairy cows based on improved Mask R-CNN. Journal of South China Agricultural University, 2020,41(06):161-168.

[14] Zhao W., Cheng X., Zhao Z., and Zhai Y., 2020. Insulator recognition based on attention mechanism and Faster RCNN. CAAI Transactions on Intelligent Systems,2020,15(01):92-98.

[15] Huang Z., Huang L., Gong Y., Huang C. and Wang X., 2019. Mask Scoring R-CNN. 2019 IEEE/CVF Conference on Computer Vision and Pattern Recognition (CVPR). IEEE, 2019.